

# Acoustic Wave Propagation in Microfluidic Application with Hierarchical Finite Element

\*X. Meng<sup>1</sup>, J. Reboud<sup>1</sup>, C.J. Pearce<sup>1</sup> and Ł. Kaczmarczyk<sup>1</sup>

<sup>1</sup> School of Engineering, Rankine Building, The University of Glasgow, Glasgow, G12 8LT, UK

\*E-mail: m.xuan.1@research.gla.ac.uk

## ABSTRACT

In this paper, we introduce a new computational method for the analysis of fluids subjected to high frequency mechanical forcing. We focus attention on surface acoustic wave droplet microfluidics. In these problems, we distinguish three time scales 1) the fast ( $\mu s$ ) time scale of Rayleigh waves on the solid surface, 2) medium ( $\mu s$ - $ms$ ) time scale of acoustic wave in the fluid droplet, and 3) slow ( $ms$ - $s$ ) time scale of capillary wave propagation on the fluid-air surface. Finite element modelling of such problems has been limited in its ability to handle the broad range of timescales. In particular, direct time integration techniques are computationally expensive because of the need to resolve the smallest timescale.

Here we solve the Helmholtz equation in the frequency domain, applying hierarchical finite element approximation based on unstructured meshes [2], where both pressure field and geometry are independently approximated with arbitrary and heterogeneous polynomial order. We demonstrate convergence of the numerical scheme and illustrate model performance using the example of a surface acoustic wave actuation of a droplet, which has applications in microfluidics and microrheology at high frequency.

**Key Words:** *acoustic modelling ; polychromatic waves ; discrete Fourier transform ; hierarchical shape functions*

## 1. Introduction

Acoustic problems have a wide range of uses in different physical applications, albeit numerical results can suffer from poor resolution and be computationally expensive. Here we focus on the development of a computational tool to aid the design of acoustic diagnostic devices (lab-on-a-chip). To avoid the need of solving the 4D wave equation, the problem is expanded to polychromatic waves via discrete Fourier transformation in both the spatial and frequency domain with respect to the input signal, solving the 3D Helmholtz equation instead. As shown in Figure 1b, it is presumed that the computational domain of a droplet (shown in purple) is a hemispherical shape with contact angle 90 degree. A surface acoustic wave (SAW) passes along a substrate that then interacts with the droplet. To determine the boundary conditions (BCs) on the droplet, the incoming Rayleigh waves are expressed as a closed form analytical equation based on developments from [3] and [4] (Figure 1a). A Fourier transform is then applied to the analytical equation to establish the BCs. This allows us to solve for the propagation of the acoustic waves in the fluid droplet in the frequency domain. This yields the pressure and velocity fields in the fluid which serves to calculate the radiation acoustic forces. These forces can be applied to solve the problem in the slow time scale using a direct time integration of Navier Stokes equation for droplet, specifically taking care of the surface tension. This final part of the problem is strongly nonlinear as a result of the evolving droplet geometry; thus, the calculations of the acoustic wave in the fluid droplet are repeated for each time step at the slow time scale.

Initially, the problem of a plane wave impinging on the sound hard surface of a cylinder is considered, where solution convergence is studied for both geometry and multiple physical fields. Moreover, error estimators and the numerical efficiency of the *hp*-adaptivity in the context of the Helmholtz equation is investigated. The application of hierarchical finite element approximation improves the computational efficiency and accuracy of the acoustic solver [2]. Subsequently, the problem of SAW actuation of a fluid droplet is considered. The proposed finite element technology is implemented in the open-source finite element University of Glasgow in-house parallel computational code, MoFEM (Mesh Oriented Finite Element Method).

## 2. Model components

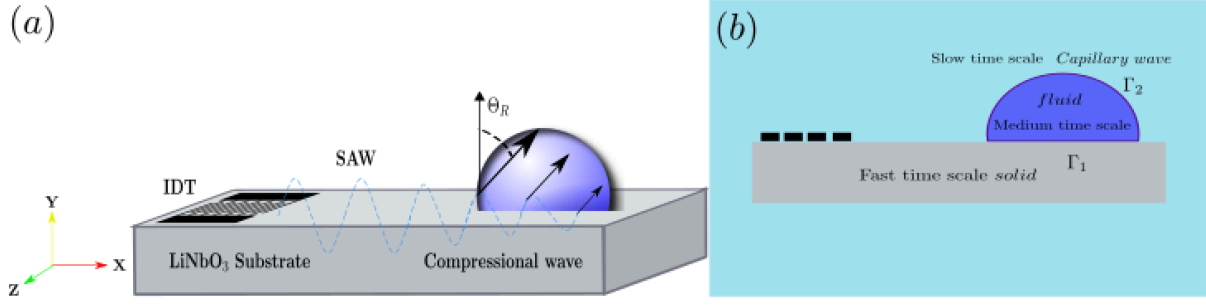


Figure 1: Surface acoustic waves application. (a) SAW actuation of a liquid drop on a LiNbO<sub>3</sub> piezoelectric surface, showing the leaky Rayleigh waves in the drop. (b) Illustration of the different timescales.

### 2.1. Boundary conditions

Let  $\Omega$  be a domain in  $\mathbb{R}^3$  with the smooth boundary and outward unit normal  $n$ . The complete form of Helmholtz equation for the acoustic problem is defined as

$$\nabla \cdot \nabla \Phi(\mathbf{r}) + k^2 \Phi(\mathbf{r}) = f(\mathbf{r}) \quad \text{in } \Omega \quad (1a)$$

$$\left( \frac{\partial \Phi(\mathbf{r})}{\partial n} + i\sigma \Phi \right) = g \quad \text{on } \Gamma \quad (1b)$$

$$\Phi = \Phi_S + \Phi_I \quad (1c)$$

where  $\Phi$  is the total acoustic potential, ( $\Phi_S$  and  $\Phi_I$  denote radiation and incident wave respectively) and the variation of  $f(\mathbf{r})$  in (1a) can be regarded as a point source of acoustic wave. (1b) shows the mixed BC with constant  $\sigma$  and  $g$ , which can be used to describe any BCs by modifying the parameters. If  $g = 0$ , the Robin BC can be either Dirichlet or Neumann BC in extreme cases.  $\sigma = \rho c$  is called the dimensionless admittance coefficient. When  $\sigma \rightarrow \infty$  the boundary is soft, conversely, when  $\sigma \rightarrow 0$ , the boundary becomes rigid [1].

### 2.2. Application on microfluidics

Rayleigh waves are a type of surface wave first proposed by Lord Rayleigh (1887), it is propagating along a free surface and the amplitude decays exponentially away from the surface. Rayleigh wave consist two types of surface acoustic waves, their potentials are: longitudinal wave  $\varphi$  and transverse wave  $(0, \psi, 0)$ . The closed form solution of Rayleigh waves on solid surface is given by

$$\varphi = A_0 e^{-q|y|} e^{ikx} \quad (2a)$$

The attenuation coefficients in analytical form are:

$$q^2 = k^2 - k^2 \frac{c_s}{c_l} > 0 \quad (3a)$$

where  $k = \frac{\omega}{c_s}$  and  $c_s$  is the phase velocity (speed) of Rayleigh wave ( $c_s = c_L$  for leaky Rayleigh wave),  $c_l$  denotes the speed of longitudinal wave on solid surface.

As illustrated in Figure 1(a) when SAW pass beneath droplet, it leaks energy into droplet, this phenomena is called the leaky SAW. In addition, longitudinal waves propagate into the droplet, with a complex wavenumber  $k_L = k + ik_i$  and speed  $c_L$ , form Rayleigh angle  $\Theta_R = \arcsin(\frac{c_l}{c_s})$  with horizontal axis. In [4], the leaky SAW number  $k_i = 2768$  for Y-X LiNbO<sub>3</sub> is provided.

### 2.3. Polychromatic wave

The detailed procedures devised to treat the case of polychromatic waves are shown in Figure 2.

$$\begin{cases} \text{Find } u \in H^1(\Omega), & \text{such that} \\ \alpha(u_{k_n}, v_{k_n}) = \hat{f}(v_{k_n}) & \forall v_{k_n} \in H^1(\Omega) \end{cases}$$

where  $\alpha(\cdot, \cdot)$  is the symmetric bilinear form based on  $H^1(\Omega) \times H^1(\Omega)$  ( $u_{k_n}$  is the finite element solution of  $\Phi_S(k_n)$ ) expressed as

$$\alpha(u_{k_n}, v_{k_n}) = \int_{\Omega} \nabla u_{k_n} \nabla v_{k_n} d\Omega - k^2 \int_{\Omega} u_{k_n} v_{k_n} d\Omega \quad (4a)$$

$$+ \sigma_1 \int_{\Gamma_2} u_{k_n} v_{k_n} dS + \sigma_2 \int_{\Gamma_1} u_{k_n} v_{k_n} dS \quad (4b)$$

$$\hat{f}(v_{k_n}) = \int_{\Omega} f v_{k_n} d\Omega + (\Phi_I(k_n) + \frac{\partial \Phi_I(k_n)}{\partial r}) \int_{\Gamma_1} v_{k_n} dS \quad (4c)$$

where  $\sigma_1$  and  $\sigma_2$  are admittance coefficients corresponding to surfaces  $\Gamma_1, \Gamma_2$ . The system of linear equations required to be solved

$$\mathbf{K}_n \mathbf{U}_n = \mathbf{F}_n \quad (5)$$

this equation is solved for  $n$  frequency where  $n$  frequencies is considered here. Once the results are computed, we then apply the inverse Fourier Transform to transfer the acoustic potential back to the time domain. With that at hand, we can calculate radial stress where it drives fluid into motion at the slow time scale. The radial stress is calculated from acoustic potential by averaging velocities [5].

### 3. Computational procedure and results

a

In the pre-processor, a parameterised geometry with uniform mesh containing tetrahedras is made in Cubit. Problem is solved using Multifrontal Massively Parallel sparse direct Solver (Mumps). In this work, hierarchical Legendre type shape functions are used. The  $l_2$  norm of solution error is calculated for different approximations and various frequencies, plots of convergence analysis were compared.

Figure 3(a) shows the absolute acoustic potential of computational domain around the hard cylinder. Figure 3(b) and (c) present the convergence of the relative error. In 3(b) the polynomial order  $p$  is fixed to 2, the mesh size  $h$  is gradually decreased. In 3(c) we increase approximation order from 1 to 7 but keep the mesh density constant.

In Figure 3(d) and (e), we have absolute acoustic pressure and radial stress for micro-droplet with 440966 number of degrees of freedoms (DOFs) and 4th order polynomials, and in Figure 3(f) the values of stress components on nodes along x-axis are plotted.

As we can notice from the plots (b), (c) of Figure 3, the convergence speed of  $p$  enrichment is nearly two times faster than  $h$  refinement. Notably, the convergence speed of relative error in plot (c) started to decrease up to certain percentages ( $k=3, 5, 10, 0.44\%, 0.32\%, 0.26\%$  respectively), this reveals the fact

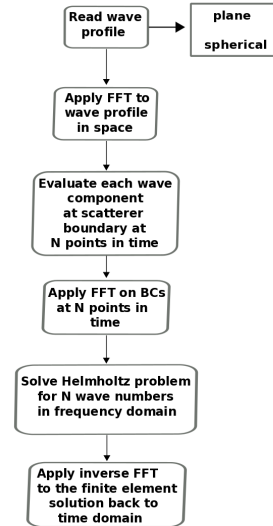
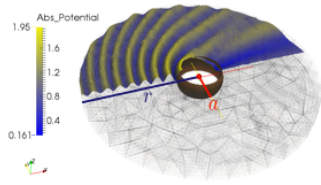
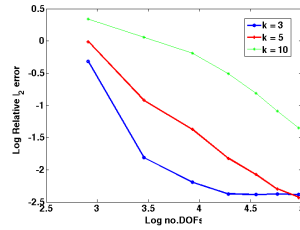


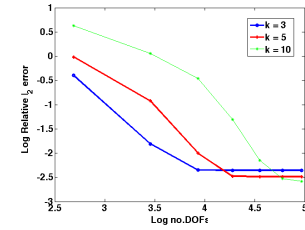
Figure 2: Diagram of polychromatic wave problem solved by Helmholtz equation



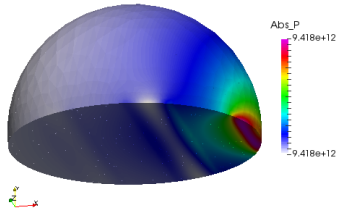
(a) Solution for hard cylinder with coarse mesh,  $p = 2$



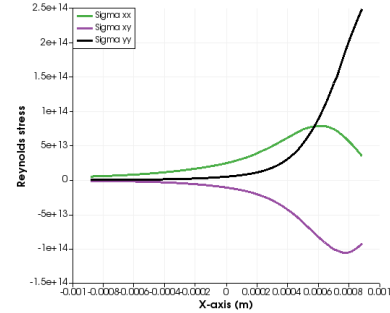
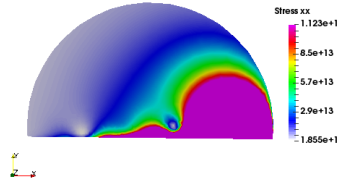
(b) Relative error of h convergence analysis in  $l_2$  norm for impinging cylinder ( $a=0.5$   $r=4$ )



(c) Relative error of p convergence analysis in  $l_2$  norm for impinging cylinder ( $a=0.5$   $r=4$ )



(d) SAW actuation of droplet with diameter & SAW width 0.002 m, RF stress  $\sigma_{xx}$  in droplet power 14dBm, 5.3 MHz frequency,  $t = 1.2830e-07$  s out of  $1.8868e-07$  s



(e) Cross-sectional of x-y plane radial stress in droplet (f) Plot data over x-axis of radial stress in droplet

Figure 3: Numerical results

that the remaining error could be due to non-reflection BC. This errors can be minimised by increasing the domain of computation or implementing exact BCs.

In Figure 3-(d)&(e) the distribution of acoustic pressure and radial stress of droplet is presented [3], the energy of LSAW is attenuated with height and distance travelled. the radial stress derived from pressure can be further employed as the input source stress into separated microfluidic equations in future research.

#### 4. Conclusions

A computational framework for polychromatic waves based on the time dependant Helmholtz equation is described for microfluids applications. In this paper we show that improving solution quality by increasing approximation order is more efficient than making mesh denser. Moreover we calculated radial stresses in droplet subjected to Leaky SAW.

#### References

- [1] Ihlenburg, F. Finite element analysis of acoustic scattering, *Springer Science & Business Media*, Vol. 132. 2006.
- [2] Ainsworth, M. & Coyle, J. Hierarchic finite element bases on unstructured tetrahedral meshes. *International journal for numerical methods in engineering*, 58(14), 2103-2130. 2003
- [3] Reboud, J., Bourquin, Y., Wilson, R., Pall, G.S., Jiwaji, M., Pitt, A.R., Graham, A., Waters, A.P. & Cooper, J. M. Shaping acoustic fields as a toolset for microfluidic manipulations in diagnostic technologies. *Proceedings of the National Academy of Sciences*, 109(38), 15162-15167. 2012
- [4] Vanneste, J., & Buhler, O. Streaming by leaky surface acoustic waves. *In Proceedings of the Royal Society of London A: Mathematical, Physical and Engineering Sciences*, (Vol. 467, No. 2130, pp. 1779-1800). The Royal Society. 2011
- [5] Lighthill, J. Acoustic streaming. *Journal of sound and vibration*, 61(3), 391-418. 1978